Analyses on the strain-rate dependent fracture behaviour of PMMA for stochastic simulations

M. Berlinger[1], P. Schrader[1], S. Kolling[1]

[1]Institute of Mechanics and Materials, Technische Hochschule Mittelhessen, Gießen

1 Introduction

Since acrylic glass, also known as poly(methyl methacrylate) (PMMA), is much lighter than conventional mineral glass, the integration into automotive structures provides weight saving that reduces the car's energy consumption. At the same time, it is a material which behaves, like mineral glass, highly stochastic in its strain at failure. That complicates a predictive simulation of structural parts, which is usually based on assumed deterministic values. In this work, the strain-rate dependent fracture strain distribution of PMMA is determined experimentally and adopted as failure criterion in the simulation of a pedestrian head impact on an automotive side rear window. Thus, the Head Injury Criterion (HIC) receives its very own distribution, showing the relevance of stochastic simulation.

2 Experimental Research

2.1 Head Impact Test

In laboratory experiments a head impact test is performed. An image series of this experiment is illustrated in Fig.1. The test is based on the New Car Assessment Programme (NCAP), choosing a child head-form impactor due to the side windows comparatively small size. The impact of the dummy head on a defined point on the screen occurs with a velocity of 10 m/s. The side window itself is made of monolithic PMMA with 4 mm thickness. Note that this test has been performed for FE validation only and is not an official standard test on the NCAP.

Fig.1: Image series of a head impact on automotive side window out of PMMA with t = 4 mm [4]

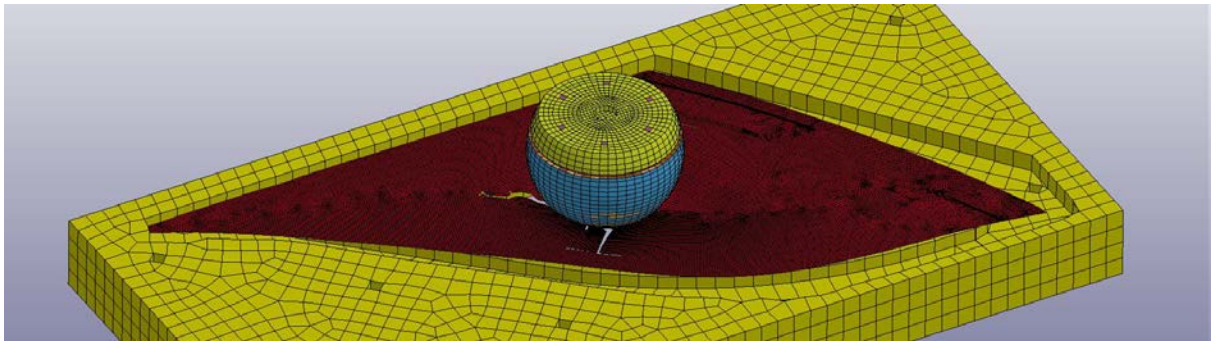

Fig.2: Simulation model of the head impact [4]

The experiment was also considered in the validation studies of Lopez Ruiz [3] for the viscoelastic PMMA model by Rühl [4,5] that uses ***MAT_GENERAL_VISCOELASTIC** in LS-DYNA. Comparing the resultant acceleration of the head impactors centre of gravity over time, their simulation shows a high concordance with the real head impact, as Fig.3 states. To this point, the simulation bases on an

assumed deterministic fracture criterion, hence the scattering strength of the material is not considered and one distinct HIC value is generated. In the following studies, a simplified simulation model by [4] is adopted using the validated material card. A snap-shot of this model after fracture is given in Fig.2.

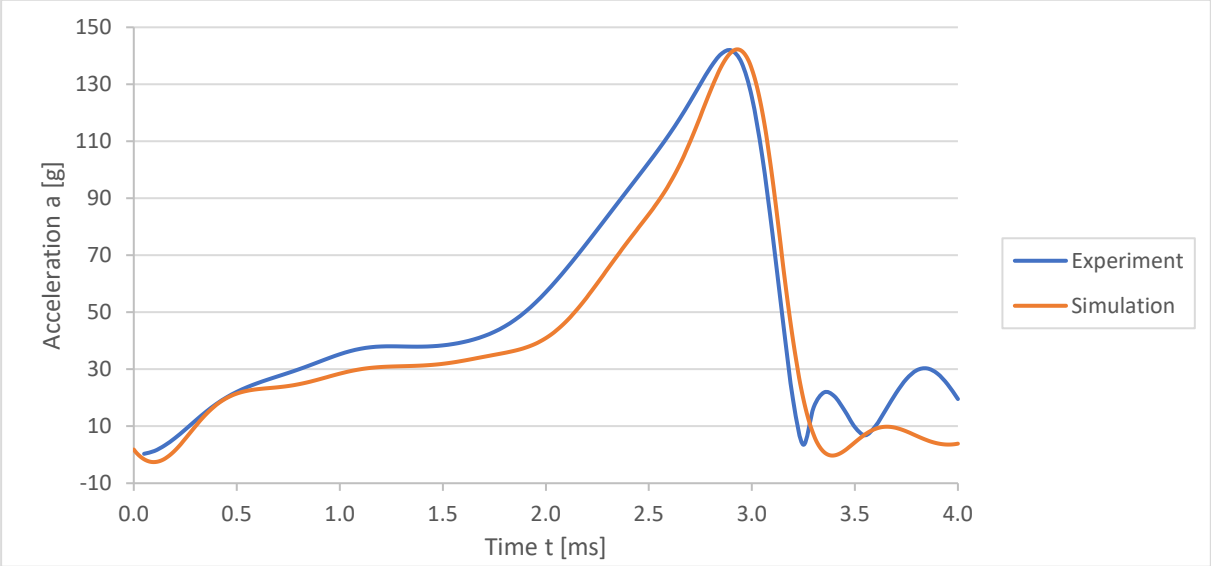

Fig.3: Experimental vs. simulative results of the head impact [3]

2.2 Tensile Tests

In order to detect the fracture strains of PMMA dependent of the strain rate, tensile tests are performed at traverse velocities of 1E0 m/s, 1E-1 m/s, 1E-2 m/s, 1E-3 m/s, and 1E-4 m/s with at least 45 repetitions for each velocity. A strain rate optimized tensile specimen geometry BZ according to [2] is chosen, which dimensions are shown on the left-hand side of Fig.4. For an understanding of the stress states inside the BZ specimen, a quasi-static tensile test is simulated with shell elements using ***MAT_GENERAL_VISCOELASTIC**, see [4] for parameter identification. On the right of Fig.4 the distribution of stress multi-axiality is visualized. The factor of multi-axiality *m*, also referred to as triaxiality, is defined as the quotient of negative hydrostatic pressure and von-Mises stress by

$$m = -\frac{p}{\sigma_{vm}} = \frac{\frac{1}{3}(\sigma_1 + \sigma_2 + \sigma_3)}{\sqrt{\frac{1}{2}[(\sigma_1 - \sigma_2)^2 + (\sigma_2 - \sigma_3)^2 + (\sigma_3 - \sigma_1)^2]}}. \quad (1)$$

For pure unaxial stress the stresses in cross and thickness direction become zero and hence *m* takes a value of 0.33. The results on the right of Fig.4 show few areas of pure uniaxial stress. Especially above and below the measuring zone an increased multiaxiality occurs. Even right in the specimens centre a uniaxial stress is only approximately achieved. Hence the fracture strains are taken punctually with slight edge distance right on the level of crack initiation, where *m* tends to values between 0.33 and 0.35.

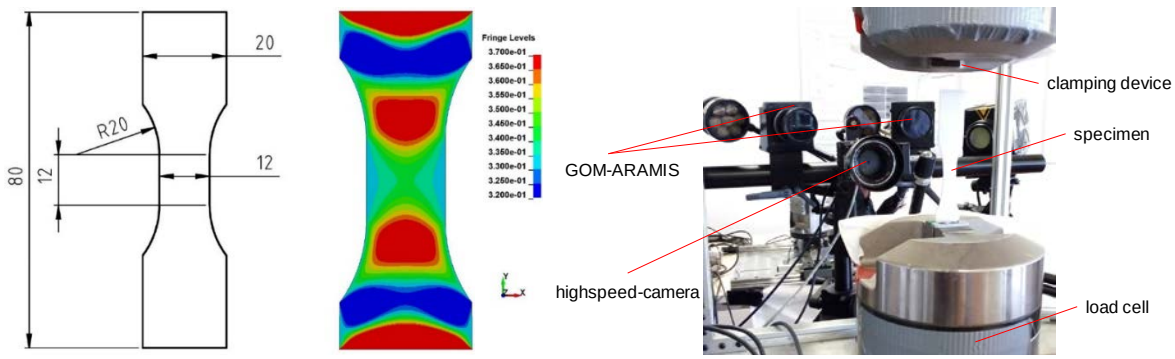

Fig.4: Dimensions of BZ tensile specimen (left), distribution of multiaxiality (middle), test setup (right)

The test setup is depicted on the right-hand side of Fig.4. It consists of a servo-hydraulic testing machine with integrated load cell, an external 3D GOM-ARAMIS system for the quasi-static tests and an additional highspeed-camera for a higher accuracy of the strain at failure. The local strain measurement is performed via digital image correlation (DIC) analysis. An example is given in Fig.5, showing the strain distribution over the specimen's surface for a quasi-static tensile test. The fracture strain is taken one picture before failure on the crack's initiation point. An error is made, since no strain information is received for the time between these two pictures when the actual failure occurs, but using the highspeed-camera, the gap is minimized by correspondingly high recording frequency. The crack starts from the edge of the specimen in the tip of the V-shaped fracture pattern. Damage by the milling process of the specimens increase the notch effect in this area, for which reason the surface strength of the material should be slightly higher. Noticeable are the hardly visible plastic strain and in contrast the blast-out of material due to the PMMAs brittleness.

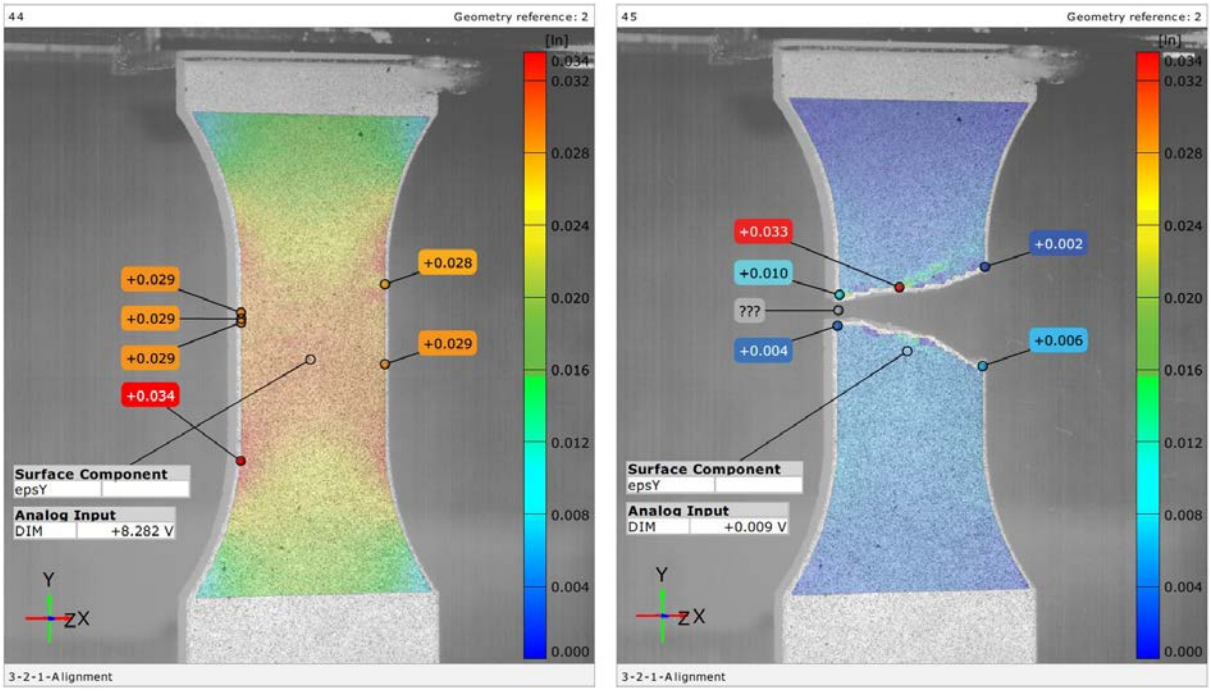

Fig.5: DIC analysis on PMMA tensile specimen one picture before failure (left) and one right after (right)

The high reproducibility of the test is indicated in the force-displacement progression measured at the traverse, which is illustrated in Fig.6. The curves nearly follow the same path, only the point of failure scatters in a wide range. That observation gives the necessity for a varying fracture criterion in the simulation of PMMA, since a deterministic value is obviously not appropriate. Beside the measuring of fracture strains, also the strain rate at the point of failure is determined through the DIC analysis. The strain rate dependent samples of fracture strain are the basis for statistical analysis.

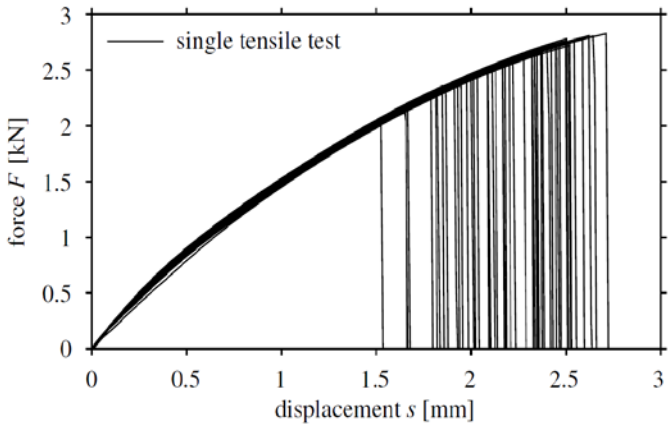

Fig.6: Force-displacement progression of quasi-static tensile tests on PMMA

3 Statistical Analyses

3.1 Distribution Fit

The DIC analyses of the performed tensile tests provide five samples of fracture strains, each one for a certain strain rate. At this point, the occurrence probability for a respective fracture strain in a sample is not known. To overcome this problem, common practice is to utilize a so-called probability estimator. For this, the *n* fracture strains within a sample are sorted in ascending order. Then, the occurrence probabilities are calculated in dependence of the position *i* in the sorting. In the scope of this work the estimator according to Weibull

$$p_i = \frac{i}{n+1} \tag{2}$$

is chosen, since it is one the rather conservative ones [1]. The pairing of fracture strain and occurrence probability is in the following referred to as plotting position. Now, on the plotting positions of one sample cumulative distributions functions (CDF) of several distribution functions are fitted and tested for their goodness of reproducing the measured data. Proved to be the best choice is the 2-parameter Weibull distribution. The results for three of the five samples are shown in Fig.7. Two were left out in this diagram for a better visualization.

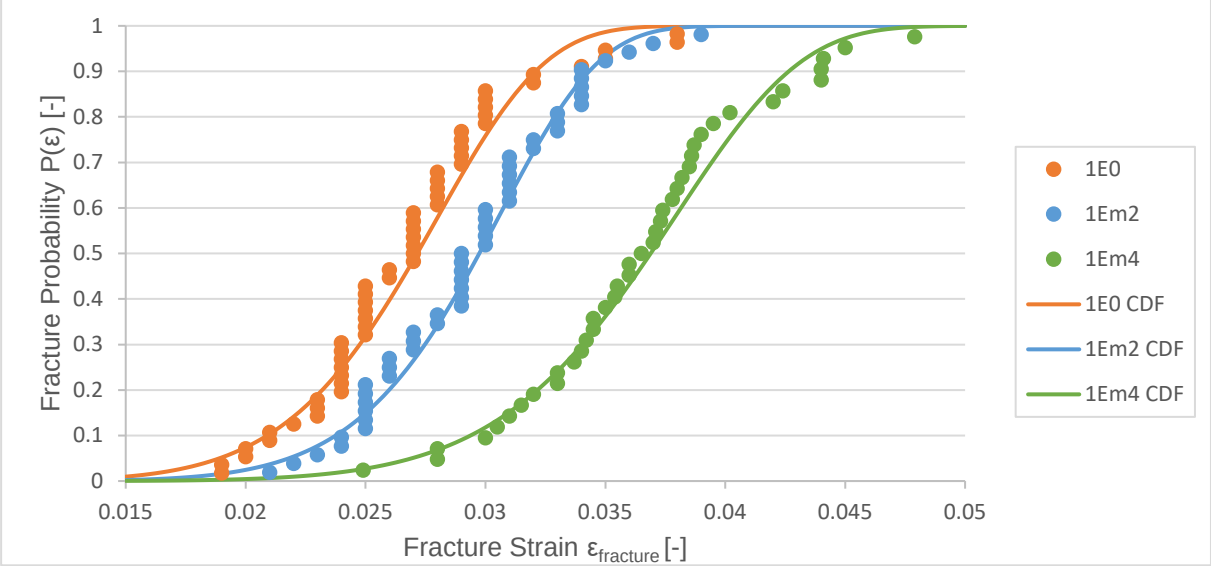

Fig.7: Fracture strain distribution of PMMA tested at various traverse velocities with respective fit of the 2-parameter Weibull distribution

The CDF of a distribution function is the integration of its probability density function (PDF). For example, in case of normal distribution the PDF is the characteristic bell-shaped curve. The PDF of a 2-parameter Weibull distribution is defined as

$$p(\varepsilon) = \frac{\beta}{\eta}\left(\frac{\varepsilon}{\eta}\right)^{\beta-1} \exp\left[-\left(\frac{\varepsilon}{\eta}\right)^{\beta}\right], \tag{3}$$

where β is the shape and η is the scale parameter. The corresponding CDF is gained by integration of Eq.(3) to

$$P(\varepsilon) = 1 - \exp\left[-\left(\frac{\varepsilon}{\eta}\right)^{\beta}\right]. \tag{4}$$

The fit of a Weibull distribution can be performed by linear regression using the so-called Weibull plot. Thus, the axes of the CDF plot are transformed by

$$y = \ln[-\ln(1-P)] \text{ and}$$
$$x = \ln(\varepsilon)\,, \tag{5}$$

bringing the 2-parameter Weibull CDF into the linear form

$$\ln\{-\ln[1-P(\varepsilon)]\} = \beta\ln(\varepsilon) - \beta\ln(\eta)\,, \tag{6}$$

what conforms with the expression $y = ax + b$. That produces the plot in Fig.8, which shows the identical CDFs and plotting positions as Fig.7. The colours in Fig.7 and Fig.8 are consistent. Both diagrams indicate the high strain rate dependency of the fracture strain. The faster the traverse velocity, i.e. strain rate of the specimen, the less strain leads to failure. The scattering of the fracture strains is quite similar.

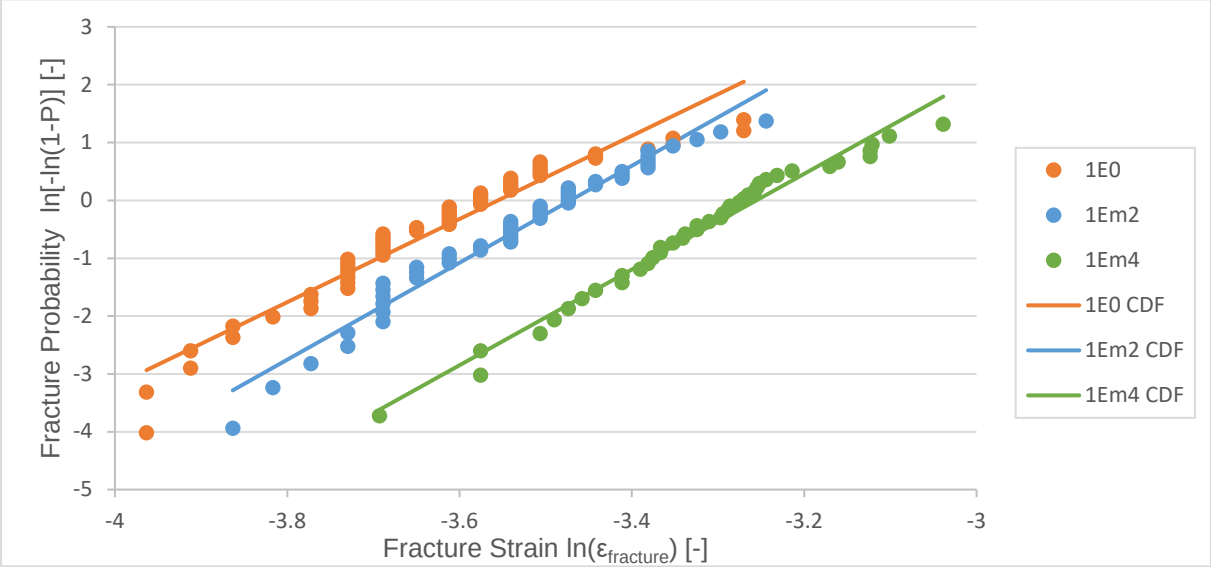

Fig.8: The fracture strain distribution plotted on Weibull axes

3.2 Simulation Input

Hitherto, five traverse velocities, i.e. five strain rates, were experimentally tested and statistically analysed. Though, for a universally valid simulation model fracture strains must be received for arbitrary strain rates. Thus, for each of the five fitted 2-parameter Weibull distributions the 5 % and 95 % quantiles are determined. Therefore Eq.(4) is solved for ε to

$$\varepsilon(P) = \eta[-\ln(1-P)]^{1/\beta} \tag{7}$$

with P once set to 0.05 and once to 0.95. The ten gained quantiles are plotted over the strain rate logarithmic to the base ten, leading to the plot in Fig.9. In doing so, the 5 % and 95 % quantiles show each a linear trend. Now, for a continuous interpolation between the tested strain rates and an extrapolation to lower and higher rates a linear regression curve for 5 % quantiles and one for 95 % quantiles is determined. Thus, by given a strain rate both quantiles can be estimated. Fortunately, for the fit of both parameters of a 2-parameter Weibull distribution minimum two quantiles are necessary, so with the 5 % and 95 % quantiles known β and η are distinctly defined. Consequently, dependent on the current strain rate the described approach provides the corresponding 2-parameter Weibull distribution of fracture strains.

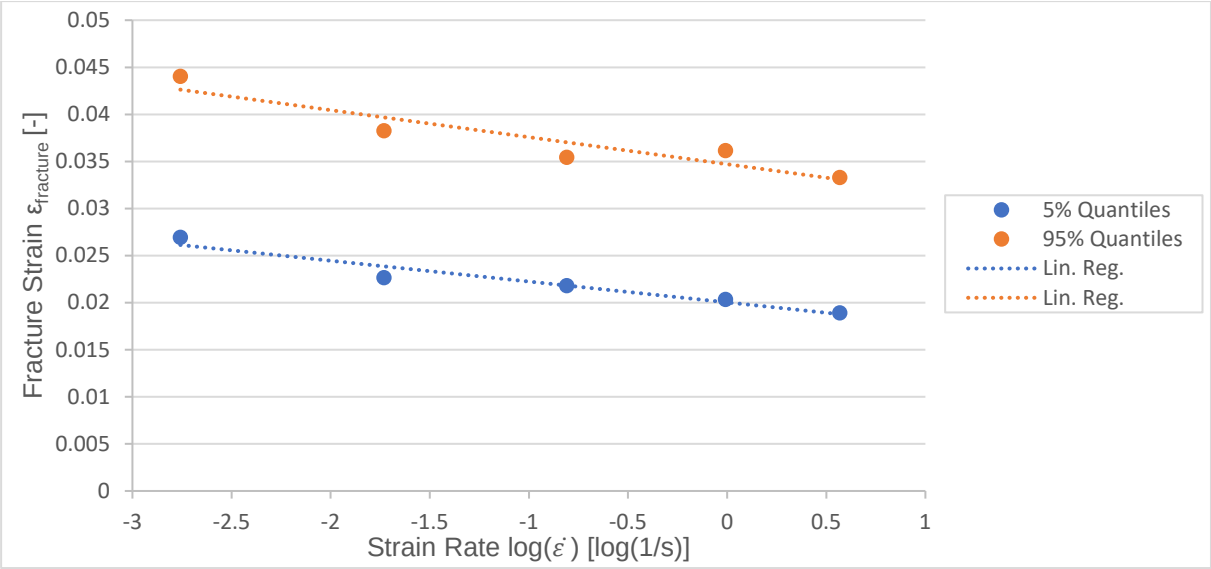

Fig.9: 5 % and 95 % quantiles of the fracture strain distribution over the respective strain rate logarithmic to the base 10

4 Head Impact Simulation

4.1 Stochastic Simulation

To add a failure criterion to the introduced ***MAT_GENERAL_VISCOELASTIC** model for PMMA, the card ***MAT_ADD_EROSION** is used additionally. As a failure criterion we use the maximum major strain dependent on the current strain rate. Reference values for these critical strains are provided by a ***DEFINE_CURVE** card for rates in ascending power of ten from 1E-7 to 1E2. For a stochastic simulation these critical strains are also set dependent on the fracture probability. That means, varying variable is the fracture probability, which is produced by a random number generator with uniform distribution. Based on the strain rate dependent 2-parameter Weibull distribution gained by the approach of the previous section, using the inverse transform sampling fracture strains are generated out of these fracture probabilities.
For example: a random number generator provides a fracture probability of 0.99. The corresponding fracture strain is determined following Eq.(7), in which β and η are calculated respective for the ten reference rates to

```
$---+----1----+----2----+----3----+----4----+----5----+----6----+----7----+----8
*DEFINE_CURVE_TITLE
Erosion epsmaj
$     lcid      sidr       sfa       sfo      offa      offo    dattyp
       300         0  1.000000  1.000000
$                a1                  o1
             1.0e-7            0.057379
             1.0e-6            0.054433
             1.0e-5            0.051488
             1.0e-4            0.048544
             1.0e-3            0.045601
             1.0e-2            0.042659
             1.0e-1            0.039719
             1.0000            0.036782
             1.0e+1            0.033848
             1.0e+2            0.030919
$---+----1----+----2----+----3----+----4----+----5----+----6----+----7----+----8
```

With this ***DEFINE_CURVE** card the head impact is then simulated in LS-Dyna and analysed with LS-PrePost. Resultant in this example is a HIC of 3003. Afterwards the procedure is started again, but with a new random fracture probability. In sum the simulation is repeated 100 times, each time with a new

random fracture probability. Thus, through many simulations with varying fracture probability a corresponding HIC distribution is gained.

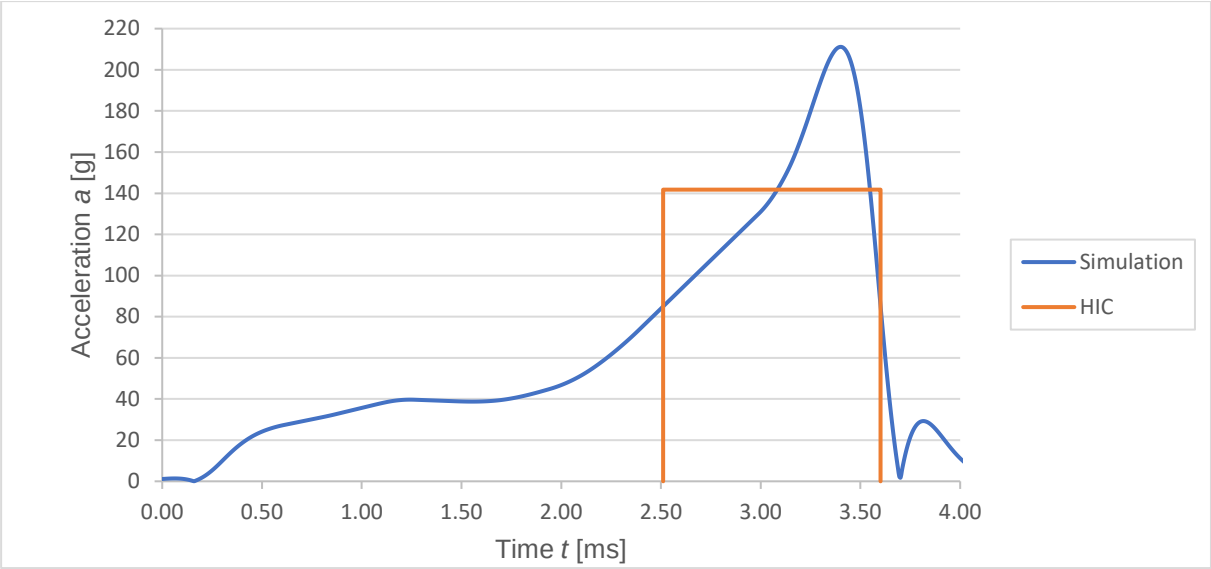

Fig.10: Acceleration over time in one of the stochastic simulations and with reference curve for the determined HIC

For HIC determination the resultant acceleration at the centre of gravity of the head impactor is analysed. The acceleration signal is filtered according to SAE J211 by CFC-1000. Fig.10 shows this acceleration as multiple of the gravitational acceleration over termination time. The HIC is calculated by

$$HIC = \left[\frac{1}{t_2 - t_1}\int_{t_1}^{t_2} a(t)\mathrm{d}t\right]^{2.5}(t_2 - t_1)\,, \tag{8}$$

in which t_1 and t_2 are time points whose choice must lead to the maximum possible function value, i.e. HIC. In Fig.10 a saltus function in the same time limits as the HIC with equivalent integral is illustrated.

4.2 HIC Distribution

Through one hundred repetitions of the head impact simulation an adequate database of possible HICs is gained. Following the procedure in section 3.1 various distribution functions are tested for their goodness-of-fit, though the plotting points progression is not that simple to reproduce. The best fit of common distribution functions is again achieved by the 2-parameter Weibull distribution, that is now defined as

$$P(HIC) = 1 - \exp\left[-\left(\frac{HIC}{\eta}\right)^{\beta}\right]. \tag{9}$$

The fit is realized as linear regression in the Weibull plot, resulting in a coefficient of determination of $R^2 = 0.9334$. In Fig.11 the simulated HICs and the 2-parameter-Weibull CDF are illustrated on regular axes.

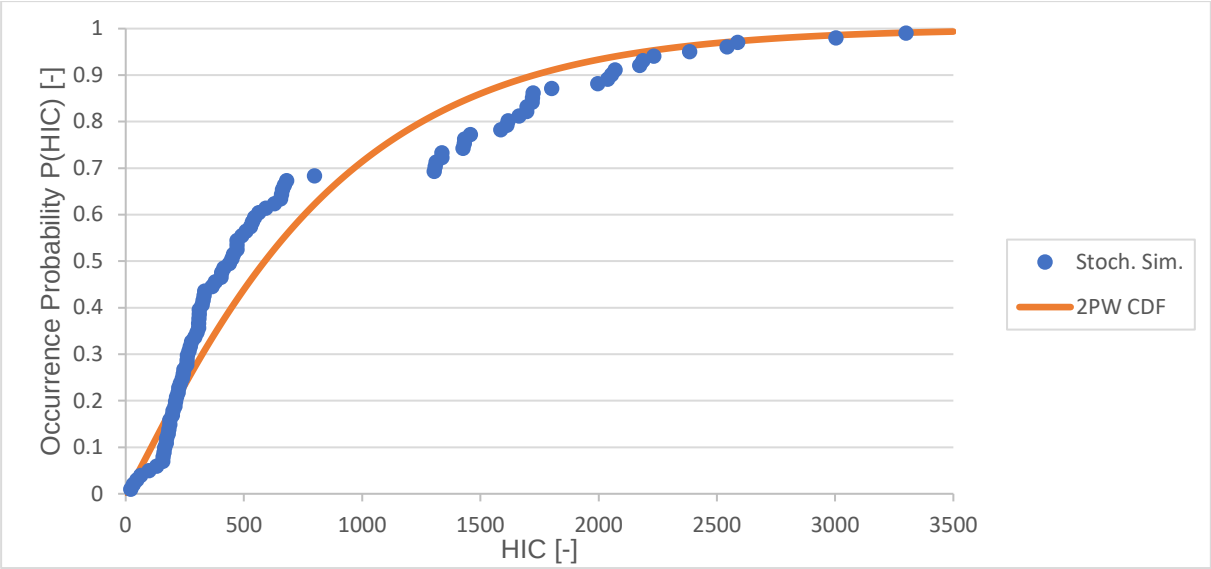

Fig.11: HIC distribution from stochastic simulation with fit of the 2-parameter Weibull distribution

The diagram in Fig.11 shows an extremely wide range of possible HICs for the determined distribution of fracture strains, with the minimum value at 21 and the maximum one at 3300. The common HIC limit of 1000 for head impact tests is exceeded in 28.6 % of the observations. At this point, further investigation of mesh dependency has to be performed.

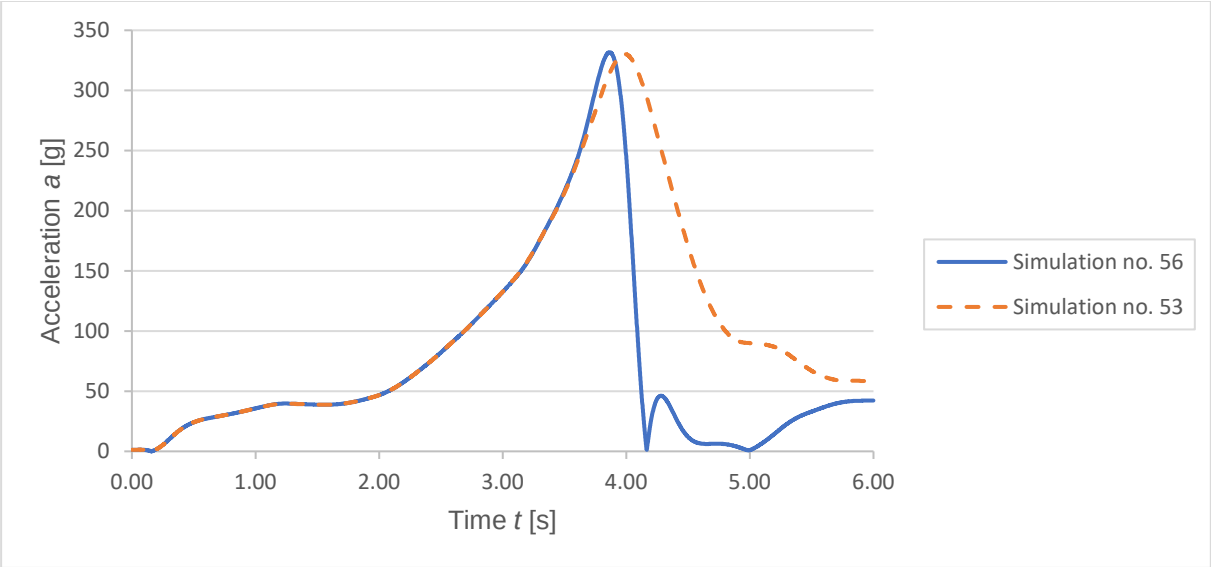

Fig.12: Differing acceleration curves despite similar failure strains

In Fig.12 the acceleration curves for two of the simulations are given. Compared to Fig.11 these are the first HIC below 1000 and the first one above. In simulation number 56 the failure strain for a strain rate of 100/s is 0.024412 and in simulation number 53 it is 0.023688. Although the failure strains are very similar, the corresponding HICs are 798 and 1305. At the begin of the head impact, both acceleration curves are identical, but right before failure, which happens at their peak, the curves diverge. Simulation number 56 fails with a rapid drop in acceleration and number 53 with a smooth transition, which causes the higher HIC. Since both simulations only differ in the load curve input in **`*MAT_ADD_EROSION`**, the observed effect must have numerical reasons belonging to the FE-mesh.

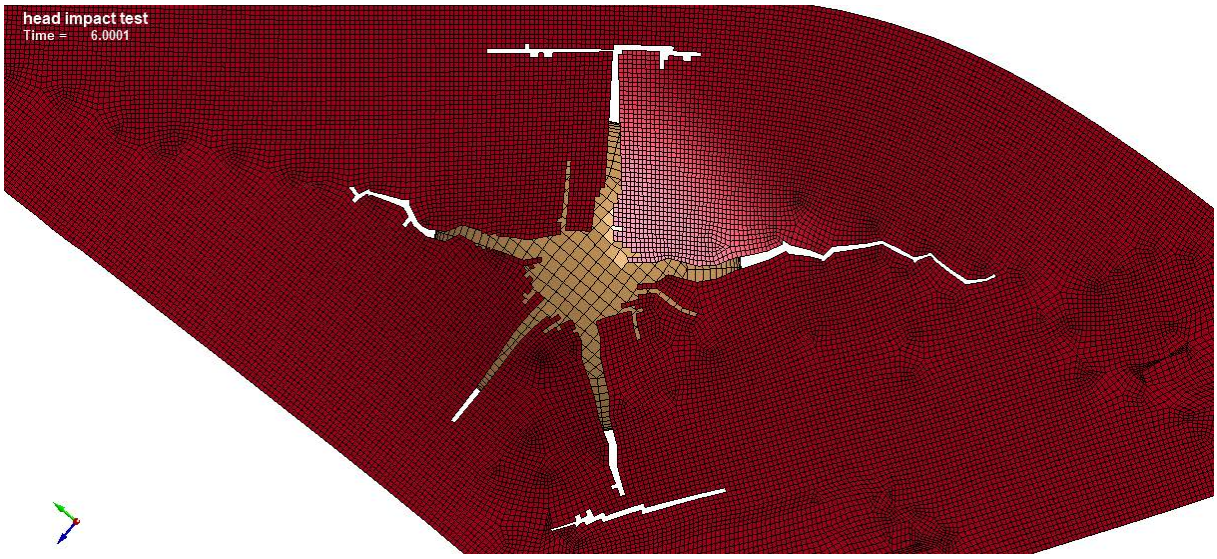

Fig.13: FE-mesh of the simulation model and resulting fracture pattern

As mentioned before in section 2.1, the analyses of this work base on a simulation model validated on a single head impact test. For this single case, the material behaviour could be reproduced very well with a discrete fracture strain. However, using a probability distribution, the model seems to be very sensitive. In Fig.13 the rather inhomogeneous FE-mesh is shown, which clearly leads the way of the crack by its element arrangement. As a result, the numerical solution seems to be influenced significantly. In future investigations, a sensitivity analysis of the model must be conducted and the FE-mesh adapted. This should achieve a correction of the HIC distribution. Nevertheless, the introduced methodology for stochastic simulations keeps its validity and is turned out as a reliable procedure for statistical analyses.

5 Summary

Acrylic glass is a material with high variability in its strength. In components this causes a major variation in fracture behaviour. Considering an automotive side rear window made of PMMA, the influence on the Head Injury Criterion (HIC) is examined. Based on a head impact test that was performed in laboratory tests for the validation of a ***MAT_GENERAL_VISCOELASTIC** model in LS-DYNA for PMMA, this work enhances the assumed deterministic failure criterion of the first approach by a consideration of stochastic material failure. In uniaxial tensile test with five different strain rates a sample is produced for a statistical analysis of the fracture strains distribution. Thus, five 2-parameter Weibull distributions are gained for the different strain rates, whose 5 % and 95 % quantiles are brought into a functional relationship, allowing to interpolate between the measured strain rates and to extrapolate to higher and lower ones. With this 5 % and 95 % quantiles for arbitrary strain rates, a respective 2-parameter Weibull distribution can be determined. Utilizing a random number generator, 100 random fracture probabilities are produced for the compilation of 100 ***DEFINE_CURVE** cards, each defining the critical major strain for reference rates in ***MAT_ADD_EROSION**. By regarding each of these failure criterions in a separate head impact simulation, a distribution of 100 different Head Injury Criterions (HICs) is gained and discussed critically.

6 Literature

[1] Ballarini, R., Pisano, G., and Royer-Carfagni, G.: The lower bound for glass strength and its interpretation with generalized Weibull statistics for structural applications, J. Eng. Mech., 142(12), 2016, 04016100.

[2] Becker, F.: Entwicklung einer Beschreibungsmethodik für das mechanische Verhalten unverstärkter Thermoplaste bei hohen Deformationsgeschwindigkeiten, Ph.D. thesis, 2009.

[3] Lopez Ruiz, D., Rühl, A., Kolling, S., Ruban, E., Kiesewetter, B., Ulzheimer, S.: CAE validation study of a side window impact using Plexiglas materials, Proceedings of the 10th European LS-DYNA Conference, 2015, pp. 229.

[4] Rühl, A.: On the time and temperature dependent behaviour of laminated amorphous polymers subjected to low-velocity impact, Ph.D. thesis, 2017.
[5] Rühl, A., Kolling, S., Schneider, J.: Characterization and modeling of poly(methyl methacrylate) and thermoplastic polyurethane for the application in laminated setups. Mech. Mat., 113, 2017, pp. 102–111.